*Research Article*

# Time-Based Separation for Aircraft Landing Using Danger Value Distribution Flow Model

## Ta-Chung Wang and Chih-Hsiang Tsao

*Institute of Civil Aviation, National Cheng Kung University, Tainan 70101, Taiwan*

Correspondence should be addressed to Ta-Chung Wang, tachung@mail.ncku.edu.tw

This study proposes a flow model using a modified Lighthill-Whitham-Richards highway model. The proposed model treats each aircraft on an airway as a continuous distribution of air collision probability, which is called the danger value distribution. With the proposed flow model, collision can be easily predicted by the peak value of the overlap of the danger value distribution of each aircraft. The study further proposes a velocity adjustment method that can be used to resolve the conflict. The proposed method can be applied for aircraft separation during the landing process, in which the separation time is different for different combinations of aircraft types.

## 1. Introduction

Currently, air travel is one of the major methods of transportation for people around the world. The rapid growth of the aviation industry has resulted in heavier air traffic. Consequently, airways and airports are both busier. Because of heavy air traffic, flight safety and air traffic management have increased in importance. To this point, air traffic management has relied on air traffic controllers (ATCs). Radar control allows ATCs to coordinate aircraft spacing directly by using visible information through the radar display. Aircraft spacing is mainly used to avoid the danger of possible collision and prevent aircraft from being affected by wake vortices induced by the preceding aircraft. The spacing can be based on time or distance. Distance-based separation is easily managed by ATCs through radar displays. However, when compared with time-based separation, distance-based separation is known to be less efficient when considering different weather conditions [1] and usage of airport capacities [2]. Owing to these disadvantages, time-based separation is commonly proposed in automatic landing sequencing algorithms [1–7]. Some time-based separations are also recommended for runway occupancy during approach and take-off

phases at airports. Although the time-based separation has several benefits over the distance-based separation, it cannot be directly observed from radar displays, making it more difficult for ATCs to use. Therefore, an automated ATC advisory system should be used to overcome this difficulty and reduce the ATCs' workload.

Air traffic flow must be modeled before it can be controlled. Along with the development of civil aviation, several evolutions in modeling air traffic flow have been proposed. In addition, concepts of modeling traffic have also evolved with the growth of air traffic flow. The Eulerian network model of air traffic is inspired by the Lighthill-Whitham-Richards (LWR) model [8–10], which was originally used for modeling highway flow. The LWR model can be numerically solved in two different ways: the Eulerian scheme and the Lagrangian scheme. Both schemes are capable of converging to the same solutions [11]. However, using Eulerian models to model air traffic flow provides several benefits over Lagrangian models [12]. First, the models are computationally tractable, and their computational complexity does not depend on the number of aircraft, but on the size of the physical problem of interest. Second, their control theoretic structure enables the use of standard methodologies to analyze them, such as control theory or optimization. Menon et al. [13] first introduced the LWR model in air traffic control to describe the density flow of air traffic. Several analyses in air traffic flow, such as controllability, reachability, and model decentralization were subsequently conducted using the LWR model with Eulerian scheme [13, 14]. The two-dimensional version of Menon model was later developed and used in predictive control of air traffic [15]. Subsequently, several other Eulerian models have been proposed. The delay system model [16] treats air traffic flow as a discrete time dynamical system, and the air traffic flow is represented by an aggregated travel time. The behavior of aircraft flows on a single link can be modeled by a deterministic linear dynamical system with unit time delay. The PDE model [17, 18] divides airspace into line elements on which the density of aircraft is modeled. By applying mass conservation to the path, the cumulative density distribution is derived as a PDE model that is represented as the relationship between spatial and temporal derivatives of density terms. The large-capacity cell transmission Model [12] uses a graph-theoretic representation of traffic flow. Air traffic flow on this graph is modeled as a discrete time dynamical system evolving on a network. Among the above-mentioned models, the PDE model incorporates the continuous dynamics of aircraft, which is close to the physics of the flows, and considers aircraft density as a continuum. Therefore, the PDE model is considered as more accurate. It has been demonstrated that the accuracy of the PDE model consistently outperforms that of the other models [12]. Therefore, in this study, the PDE model has been used to derive the flow model of the danger value distribution.

This study presents a danger value distribution flow model that captures the time-based separation characteristics, permitting its use to manage time-based separations. Using the proposed model, we can determine how crowded the airspace is and detect whether the separation between the aircraft is sufficient. Thus, the proposed model can provide more detailed separation information to ATCs. In the proposed model, different separation constraints are considered for different combinations of aircraft types, which make our method applicable for complicated separation situations during the aircraft landing process. Moreover, we have also provided an automatic speed adjustment procedure that maintains minimum separation time between aircraft and thus maximizes runway capacity.

The organization of this paper is as follows. In Section 2, we have presented the concept of the danger value distribution and the associated flow model, and in Section 3, we have discussed the automated velocity adjustment algorithm, which can be used when separation conflicts are detected. A numerical example is provided in Section 4, and finally,

the conclusion is presented in Section 5. Throughout this paper, the speed of the aircraft is represented in knots (kts) and "nm" denotes nautical miles. For reference, 1 kt = 1.852 km/h and 1 nm = 1.852 km.

## 2. Danger Value Distribution

### 2.1. Danger Value Profile

Wake vortices are turbulent airflows generated during all phases of flight as a byproduct of the wing that is generating the lift. This turbulent flow of air may cause an aircraft to undergo an unstable flight period, resulting in injuries as well as loss-of-control accidents. As aircraft get closer to each other during the landing procedure, the wake turbulence problem is especially prominent during landing, particularly for a smaller aircraft following a larger aircraft. This is because a larger aircraft may generate stronger turbulent flow than a smaller aircraft, whereas a smaller aircraft may have fewer methods of resisting the strong turbulent flow than a larger aircraft. Therefore, the ability of different types of aircraft to resist and induce vortices should be considered when developing the danger value profiles for wake avoidance separation procedure. The width and length of the area, which are influenced by the generated vortex, are related to the speed and type of the aircraft [2], and the danger value profiles are modeled to reflect these characteristics. The danger value profile preceding an aircraft represents its capability to resist turbulent flow. Higher danger values indicate a diminished ability of an aircraft to resist turbulent flow. The danger value profile behind an aircraft is the amount of turbulent flow that it generates.

For the best utilization of runway capacity, the optimum situation is that the trailing aircraft should follow the preceding aircraft by the distance specified by ICAO's separation criteria during the landing process. As there is no time-based separation rule for landing, we have used Freville's method to convert ICAO's rule to a time-based rule by assuming an average landing speed of 136 kts for all types of aircraft [1]. Table 1 provides the time-based separation regulations, which can be further refined if the average landing speeds of different types of aircraft are available.

We used a single critical value as an indicator of insufficient separation for all types of aircraft. This critical value should be higher than the peak danger value in the presence of an aircraft, and be lower than the peak danger value when two aircraft collide with each other. In our design, the danger value profile of an aircraft has a peak value of 1 located at the location of the aircraft. When two aircraft are located at the same position, which indicates a mid-air collision, the peak danger value is 2. Therefore, at the minimum time-based separation distance, the peak danger value should lie between 1 and 2. Here, we have used 1.5 as the detection value for insufficient separation to design the danger value profile. The danger value profiles preceding and following an aircraft describe the capability of an aircraft to resist and induce vortices, respectively. Figure 1 shows the concept of separation detection using the danger value profile. $T_b$ is the time in which the preceding aircraft left point $A$ on the airway. $T_a$ is the time needed for the trailing aircraft to reach point $A$. The summed time, $T_a + T_b$, reflects the separation time. Let us consider that the critical separation is detected by a danger value of 1.5. Then, the danger value of the preceding and trailing aircraft should be 0.75 at point $A$ in Figure 1. Using this concept, we can design the time of the danger value profile preceding and following an aircraft that has a danger value of 0.75, by satisfying ICAO's wake vortex separation rules.
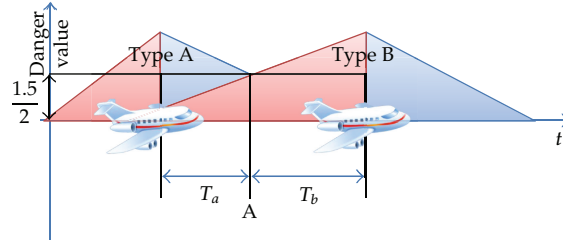
**Figure 1:** The wake vortex separation scheme.

Let the time at which the danger value is 0.75 be $T_a$ and $T_b$ for each type of aircraft, as shown in Figure 1. The variables for each type of aircraft are listed in Table 2. The following linear programming problem is employed to determine the span at both sides of the danger value profile of each aircraft.

$$
\begin{aligned}
\min \quad & \mathbf{1}^T \mathbf{x} \\
\text{s.t.} \quad & \mathbf{A}\mathbf{x} \geq \mathbf{b} \\
& x_i \geq 0 \quad \text{for } i = 1,\dots,8,
\end{aligned}
\tag{2.1}
$$

where

$$
\mathbf{A} = 
\begin{bmatrix}
1 & 1 & 0 & 0 & 0 & 0 & 0 & 0 \\
1 & 0 & 0 & 1 & 0 & 0 & 0 & 0 \\
1 & 0 & 0 & 0 & 0 & 1 & 0 & 0 \\
1 & 0 & 0 & 0 & 0 & 0 & 0 & 1 \\
0 & 1 & 1 & 0 & 0 & 0 & 0 & 0 \\
0 & 0 & 1 & 1 & 0 & 0 & 0 & 0 \\
0 & 0 & 1 & 0 & 0 & 1 & 0 & 0 \\
0 & 0 & 1 & 0 & 0 & 0 & 0 & 1 \\
0 & 1 & 0 & 0 & 1 & 0 & 0 & 0 \\
0 & 0 & 0 & 1 & 1 & 0 & 0 & 0 \\
0 & 0 & 0 & 0 & 1 & 1 & 0 & 0 \\
0 & 0 & 0 & 0 & 1 & 0 & 0 & 1 \\
0 & 1 & 0 & 0 & 0 & 0 & 1 & 0 \\
0 & 0 & 0 & 1 & 0 & 0 & 1 & 0 \\
0 & 0 & 0 & 0 & 0 & 1 & 1 & 0 \\
0 & 0 & 0 & 0 & 0 & 0 & 1 & 1
\end{bmatrix}
\tag{2.2}
$$

and $\mathbf{b} =$ [79 106 132 159 79 79 106 132 79 79 106 132 79 79 106 106]. In (2.1), $\mathbf{x} = [x_1,\dots,x_8]$ is the vector of the variables that must be solved, and 16 constraints are used to ensure that the solution satisfies the ICAO wake turbulence avoidance criteria. The optimization problem is solved with $\mathbf{x} =$ [73.7338   32.1485   47.2632   32.1485   47.2632   58.6191   47.2632   85.0897], when $\mathbf{1}^T \mathbf{x} = 432.5294$.

The separation criteria determined using linear programming are shown in Table 3. When compared with the ICAO regulation shown in Table 1, there are two significant

**Table 1:** Time-based separation criteria derived with average landing speed.

| Following aircraft (second) | Leading aircraft | | | |
|---|---|---|---|---|
| | Small | Large | B757 | Heavy |
| Small | 79 | 106 | 132 | 159 |
| Large | 79 | 79 | 106 | 132 |
| B757 | 79 | 79 | 106 | 132 |
| Heavy | 79 | 79 | 106 | 106 |

**Table 2:** Variables of different types of aircraft.

| Aircraft type | $T_a$ (sec) | $T_b$ (sec) |
|---|---|---|
| Small | $x_1$ | $x_2$ |
| Large | $x_3$ | $x_4$ |
| B757 | $x_5$ | $x_6$ |
| Heavy | $x_7$ | $x_8$ |

differences, which are shown in italic fonts. This is because we are using 8 variables to satisfy 16 constraints. Nonetheless, these differences still satisfy ICAO's criteria.

Figure 2 shows the resultant danger value profiles used during the landing process. We have different danger value profiles for different types of aircraft. As shown in this figure, larger aircraft have larger danger value spans behind them, which reflects the fact that larger aircraft induce stronger turbulent flows. Conversely, smaller aircraft have larger danger values in front of them, signifying that smaller aircraft have a lower capability to resist turbulent flow. It should be noted that these danger value profiles are all smooth curves. This is because sharp changes in the danger value lead to some undesired spikes and oscillations in the simulation result, and vibrations occur and drag the peak value. Hence, the danger value profile must descend smoothly on both sides to make its computation numerically stable.

### 2.2. Danger Value Distribution Flow Model

In this section, we introduce the modified LWR model used in air traffic control. As the arriving aircraft flows are not as dense as those on the en-route airway, one may suspect whether the LWR model, which was originally designed for modeling high-way traffic in a continuous way, is appropriate for modeling the arriving aircraft flow, which seems more discretized than high-way traffic. Our selection of the LWR model is based on various successful examples and applications in the literatures [12, 15, 16, 18]. The formulation of the modified LWR model produces a system of interconnected control volumes, which can be used to model any air traffic environment [15]. Moreover, we now represent each aircraft as a continuous distribution of danger values on the airway. Therefore, we believe that the use of the LWR model, which also treats individual vehicles with a continuous density distribution, is appropriate.

The LWR model can be numerically solved in either the classical Eulerian scheme or a Lagrangian scheme. As we had added the danger values associated with each aircraft at fixed locations, the Eulerian scheme was opted in this study. Moreover, the Eulerian scheme can be easily used for control purposes than the Lagrangian scheme [18] and was used as follows.

Table 3: The separation time using the danger value distribution.

| Following aircraft (second) | Leading aircraft | | | |
| --- | --- | --- | --- | --- |
| | Small | Large | B757 | Heavy |
| Small | *106* | 106 | 132 | 159 |
| Large | 79 | 79 | 106 | 132 |
| B757 | 79 | 79 | 106 | 132 |
| Heavy | 79 | 79 | 106 | *132* |
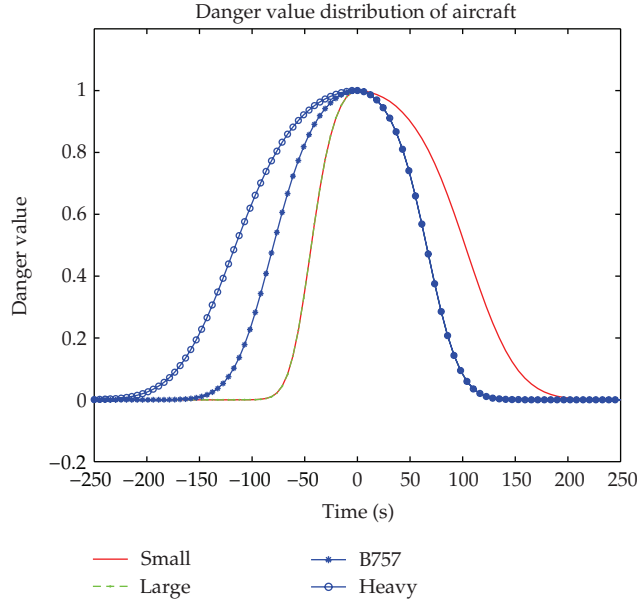


Figure 2: Danger value profiles for landing.

Let $\rho(x,t)$ be the vehicle density and $q^{\text{in}}(t)$ the inflow at the entrance of the route (i.e., at $x = 0$); the vehicle density satisfies the following PDE [17–19]:

$$\frac{\partial \rho(x,t)}{\partial t} + \frac{\partial}{\partial x}(\rho(x,t)v(x)) = 0,$$

$$\rho(x,0) = \rho_0,$$

$$\rho(0,t)v(0) = q^{\text{in}}(t),$$

(2.3)

where $\rho_0$ is the initial distribution of density on the airway. The rederived LWR PDE can also be derived from the conservation of mass. Two successive applications of the chain rule to the conservation in flow mass lead to the relation between the space derivative and the time derivative of $\rho$. That is,

$$\frac{d(\rho(x,t)v(x))}{dt} = 0.$$

(2.4)

From (2.3) or (2.4), we have $\rho_t = -\rho_x v - \rho v\prime$.

If the danger value is treated as a density distribution on the airway, its peak value decreases when the density distribution becomes wider, which is a consequence of increased velocity. This phenomenon is undesirable for time-based separation because we use the summed danger value for insufficient separation detection. To solve this problem, we designated danger value distribution flows in a velocity-related coordinate $y$, in which the velocity is constant with respect to $y$. Then we let the accumulated danger value be conserved in the $y$ coordinate, similar to the mass conservation idea in the $x$ coordinate. Using this concept, let $y$ be a function of $v(x)$ and $x$, such that $v(y)$ is constant in the $y$ coordinate. From

$$v(y) = \frac{dy}{dt}, \tag{2.5}$$

we have

$$v(y) = \frac{dy}{dx}v(x) = c, \tag{2.6}$$

where $c$ is some assumed velocity of an aircraft in the $y$ coordinate. Then,

$$v(x) = c\frac{dx}{dy}. \tag{2.7}$$

Now, let the flow be conservative in the $y$ coordinate. Thus, we have

$$\frac{d(\rho(y,t)v(y))}{dt} = 0. \tag{2.8}$$

Subsequently, the time derivation of $\rho$ in the $y$ coordinate will be $\rho_t = -\rho_y(y,t)v(y) - \rho(y,t)v_y(y)$. As $v(y) = c$, we have $v_y(y) = 0$. Hence,

$$
\begin{aligned}
\rho_t &= -\rho_y(y,t)v(y) \\
&= -\rho_y\frac{dy}{dx}v(x) \\
&= -\frac{\partial\rho}{\partial x}v(x) \\
&= -\rho_x(x,t)v(x).
\end{aligned}
\tag{2.9}
$$

This leads to a new relationship between the spatial derivation and temporal derivation as

$$\rho_t(x,t) + v(x)\rho_x(x,t) = 0. \tag{2.10}$$

We used finite difference methods to approximate the solutions of (2.10). The finite difference scheme begins with defining a grid of points in the $(x,t)$ plane. Let $h$ and $k$ be positive numbers indicating the spacing in $x$ and $t$ coordinates, respectively. The grid will be

the points $(x_m, t_n) = (mh, nk)$ for arbitrary integers $m$ and $n$. By differentiating (2.10) with respect to time, we can obtain

$$\rho_{tt} = -\rho_{xt}(x,t)v(x) - \rho_x(x,t)v_t(x), \tag{2.11}$$

where

$$\rho_{xt} = -\rho_{xx}(x,t)v(x) - \rho_x(x,t)v\prime(x). \tag{2.12}$$

The second-order Taylor series approximation of $\rho$ on the finite difference grid with respect to time is

$$\rho(x_i, t_{j+1}) = \rho(x_i, t_j) - \rho_t(x_i, t_j)k - \rho_{tt}(x_i, t_j)\frac{k^2}{2}. \tag{2.13}$$

Several numerical schemes can be used to compute the danger value distribution flow model. The Lax-Wendroff scheme [20] is often used for its ability to maintain a good pulse shape. Hence, the Lax-Wendroff scheme has been employed in the remaining part of this study. By applying the Lax-Wendroff scheme, we obtained the danger value distribution at the next time instance as

$$\begin{aligned} \rho(x_i, t_{j+1}) &= \rho(x_i, t_j) - v(x_i)\rho_x(x_i, t_j)k \\ &\quad + v(x_i)\big[v(x_i)\rho_{xx}(x_i, t_j) + v'(x_i)\rho_x(x_i, t_j)\big]\frac{k^2}{2}. \end{aligned} \tag{2.14}$$

The evolution of the danger value distribution can be written as a state function between two time steps with a transitional matrix mapping. We can rewrite (2.14) in the vector form as

$$\begin{aligned} P(t+1) &= P(t) - \mathrm{diag}(V)P_x(t)k \\ &\quad + \mathrm{diag}(V)\big[\mathrm{diag}(V)P_{xx}(t) + \mathrm{diag}(V')P_x(t)\big]\frac{k^2}{2}, \end{aligned} \tag{2.15}$$

where $P(t) = [\rho(x_1, t), \rho(x_2, t), \rho(x_3, t), \ldots, \rho(x_m, t)]^T$ is the vector of danger values at time $t$ and $V = [v(x_1), v(x_2), v(x_3), \ldots, v(x_m)]$ is the velocity profile. Other elements in (2.15) are

$$\begin{aligned} P_x(t) &= D_1 P, \\ P_{xx}(t) &= D_2 P, \\ V' &= D_1 V, \end{aligned} \tag{2.16}$$

where $D_1$ and $D_2$ are $m \times m$ matrices defined as

$$
D_1 = \begin{bmatrix}
0 & 0 & 0 & 0 & 0 & 0 & 0 \\
-1 & 0 & 1 & 0 & 0 & 0 & 0 \\
0 & -1 & 0 & 1 & 0 & 0 & 0 \\
0 & 0 & \ddots & \ddots & \ddots & 0 & 0 \\
\vdots & \ddots & \ddots & \ddots & \ddots & \ddots & \vdots \\
0 & 0 & \cdots & 0 & -1 & 0 & 1 \\
0 & 0 & \cdots & 0 & 0 & 0 & 0
\end{bmatrix},
$$

$$
D_2 = \begin{bmatrix}
0 & 0 & 0 & 0 & 0 & 0 & 0 \\
1 & -2 & 1 & 0 & 0 & 0 & 0 \\
0 & 1 & -2 & 1 & 0 & 0 & 0 \\
0 & 0 & \ddots & \ddots & \ddots & 0 & 0 \\
\vdots & \ddots & \ddots & \ddots & \ddots & \ddots & \vdots \\
0 & 0 & \cdots & 0 & 1 & -2 & 1 \\
0 & 0 & \cdots & 0 & 0 & 0 & 0
\end{bmatrix}.
$$

(2.17)

The evolution of danger values from time $t$ to time $t+1$ can be written as $P(t+1) = AP(t)$, and the change in the danger value distribution can be easily computed using $P(t + n) = A^n P(t)$, where

$$
A = I - k \operatorname{diag}(V)D_1 + \operatorname{diag}(V)^2 D_2
$$
$$
+ \operatorname{diag}(V) \operatorname{diag}(D_1 V) D_1 \frac{k^2}{2}.
$$

(2.18)

## 3. Velocity Adjustment

When insufficient time-based separation between aircraft is detected, ATCs should make necessary arrangements for the involved aircraft to avoid danger of possible collision. In this section, we present a method of velocity adjustment that maintains the minimally required separation time between aircraft so that the capacity of an airway can be optimally utilized. The proposed approach considers the case where two adjacent aircraft are flying along the same airway in the same direction at the same altitude. That is, one aircraft is chasing the other aircraft at the same flight level. If the two aircraft are traveling with the same velocity profile, the time-based separation between these two aircraft remains fixed. This idea inspired the proposed velocity adjustment procedure.

Let us assume that the preceding and trailing aircraft have danger value profiles $W_p(t)$ and $W_t(t)$, respectively. Let us set the minimum time-based separation as $T_s$ s. From Figure 1, the critical value, defined as the peak value of the danger value distribution when a time-based separation of $T_s$ s is detected, is equal to the addition of $W_p(-T_b)$ of the preceding aircraft plus the danger value at $t = T_a$ of the trailing aircraft, that is, $W_p(-T_b) + W_t(T_a)$. From our design of the danger value profile, $T_s = T_a + T_b$ and $W_p(-T_b) = W_t(T_a)$. Now, suppose that the trailing aircraft travels faster than the preceding aircraft. Eventually, the trailing aircraft will catch the preceding aircraft. The moment at which the time-based separation is $T_s$ s, at
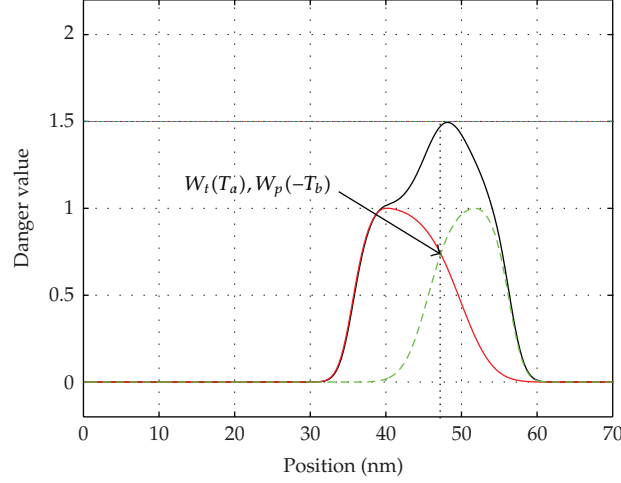
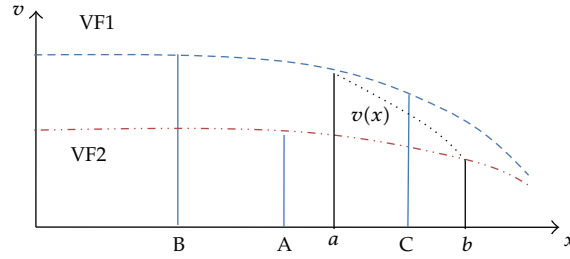**Figure 3:** Minimum time-based separation.



**Figure 4:** Velocity profiles of two aircraft.

which point the critical value is $W_p(-T_b) + W_t(T_a)$, is shown in Figure 3. We adjusted the velocity profile of the trailing aircraft so that the location of point $W_t(T_a)$ never passes point $W_p(-T_b)$ before these two aircraft reach the runway. Moreover, to maximize the utilization of runway capacity, the ideal situation is to maintain the minimum time-based separation. Therefore, we also changed the speed profile of the trailing aircraft so that the time-based separation between these two aircraft is maintained at $T_s$ s.

Consider the case shown in Figure 4. The velocity profiles of the trailing and preceding aircraft are marked as VF1 and VF2, respectively. Suppose that, at some instance prior to the occurrence of minimum time-based separation, the $W_p(-T_b)$ position of the preceding aircraft and the $W_t(T_a)$ position of the trailing aircraft are located at points $A$ and $B$, respectively. The location on the airway at which the aircraft at points $A$ and $B$ meet is marked as point $C$. Point $C$ can be determined from the simulation result of the danger value flow on the airway. The duration time needed to travel from points $A$ and $B$ to reach position $C$ can be calculated using the integral of the inversed velocity profile as follows:

$$t = \int_x \frac{dx}{v}. \tag{3.1}$$

Let us suppose that the trailing aircraft can decelerate at a deceleration speed $\alpha$ and is capable of flying with the same speed as the preceding aircraft. Using this information, we can generate a deceleration curve, $v(x)$, connecting VF1 and VF2 through intersections located at points $a$ and $b$, as shown in Figure 4. Then, the trailing aircraft can gradually change its velocity from VF1 to VF2 by passing through the connecting curve $v(x)$. To achieve minimum time-based separation, the curve must be placed such that points $A$ and $B$ reach point $b$ at the same time. That is,

$$\int_B^a \frac{dx}{\text{VF1}(x)} + \int_a^b \frac{dx}{v(x)} = \int_A^b \frac{dx}{\text{VF2}(x)}. \tag{3.2}$$

As we already know that the aircraft at points $A$ and $B$ reach point $C$ at the same time, using the original velocity profiles, we have

$$\int_B^C \frac{dx}{\text{VF1}(x)} = \int_A^C \frac{dx}{\text{VF2}(x)}. \tag{3.3}$$

From (3.2) and (3.3),

$$\int_a^b \frac{dx}{v(x)} - \int_a^C \frac{dx}{\text{VF1}(x)} = \int_C^b \frac{dx}{\text{VF2}(x)}. \tag{3.4}$$

Then, we used bisection searching by moving the curve up or down to satisfy (3.4). The algorithm for this procedure is shown as follows.

*Step 1.* Let $V_U = \text{VF1}(C)$, $V_D = \text{VF2}(C)$, and $V_p = (V_U + V_D)/2$.

*Step 2.* Let $v(x) = \sqrt{V_P^2 - 2\alpha(x - C)}$ be the deceleration curve connecting VF1 at $a$ and VF2 at $b$, where $\alpha$ is a given deceleration speed depending on the performance specification of the succeeding aircraft.

*Step 3.* Update $V_p$, $V_U$, and $V_p$ using the following rule:

$$\text{if } \int_a^b \frac{dx}{v(x)} - \int_a^C \frac{dx}{\text{VF1}(x)} - \int_C^b \frac{dx}{\text{VF2}(x)} < 0,$$

$$\text{let } V_U = V_P, \ V_p = \frac{V_p + V_D}{2},$$

$$\text{if } \int_a^b \frac{dx}{v(x)} - \int_a^C \frac{dx}{\text{VF1}(x)} - \int_C^b \frac{dx}{\text{VF2}(x)} > 0,$$

$$\text{let } V_D = V_P, \ V_p = \frac{V_p + V_U}{2}. \tag{3.5}$$

*Step 4.* Repeat Step 2 and Step 3 until

$$0 \leq \int_a^b \frac{dx}{v(x)} - \int_a^C \frac{dx}{\text{VF1}(x)} - \int_C^b \frac{dx}{\text{VF2}(x)} \leq \epsilon, \tag{3.6}$$

where $\epsilon$ is a small positive value that can be chosen according to the desired accuracy of the time-based separation. This ensures that the separation time is close to $T_s$ s but is not less than $T_s$ s.

If the speed of the preceding aircraft is so slow that the trailing aircraft cannot travel using the velocity profile of the preceding aircraft, then the only allowable location for minimum time-based separation to occur is at the end of the airway. In this situation, the velocity change curve will be used as the transition from the original velocity profile to the minimum speed, $v_m$, of the trailing aircraft. Again, the intersection of the velocity change curve and the original velocity profile will be searched, so that

$$\int_A^E \frac{dx}{\text{VF2}} = \int_B^a \frac{dx}{\text{VF1}} + \int_a^b \frac{dx}{v(x)} + \int_b^E \frac{dx}{v_m}, \tag{3.7}$$

where $A$ and $B$ are the locations defined in Figure 3 and $E$ is the location of the end of the airway. As shown in Figure 3, as the aircraft at both points $A$ and $B$ reach point $C$ at the same time following the original velocity profile, we have

$$\int_C^E \left( \frac{1}{VF2} - \frac{1}{VF1} \right) dx = \int_b^E \frac{dx}{v_m} + \int_a^b \left( \frac{1}{v(x)} - \frac{1}{VF1} \right) dx. \tag{3.8}$$

Then, we need to change the location of $v(x)$ so that the above-mentioned equation can be satisfied. In this case, it is not guaranteed that point $C$ lies between points $a$ and $b$. Therefore, the bisection search needs a wider range to find the intersection of $a$ and $b$. It should be noted that the above-mentioned algorithms and decision conditions (3.4) and (3.8) do not rely on the actual location of points $A$ and $B$. Only the predicted location of the minimum allowable separation point $C$ is required for the velocity change curve calculation.

## 4. Simulations

This section presents an example of the time-based separation using the danger value distribution flow model with the proposed danger value profiles shown in Figure 2. Figure 5 shows the velocity profiles used in this section. The solid-line curve is the velocity profile of the trailing aircraft, whereas the dashed curve is the velocity profile of the preceding aircraft. The initial positions of the trailing and preceding aircraft are located at approximately 20 and 35 nm, respectively. As the trailing aircraft is traveling at a higher velocity than the preceding aircraft, there will be insufficient time-based separation at some future point. With the danger value distribution flow model, near misses in the time-based separation can be predicted, and a new velocity profile suggestion is proposed to maintain the minimally required time-based separation until the end of the airway.
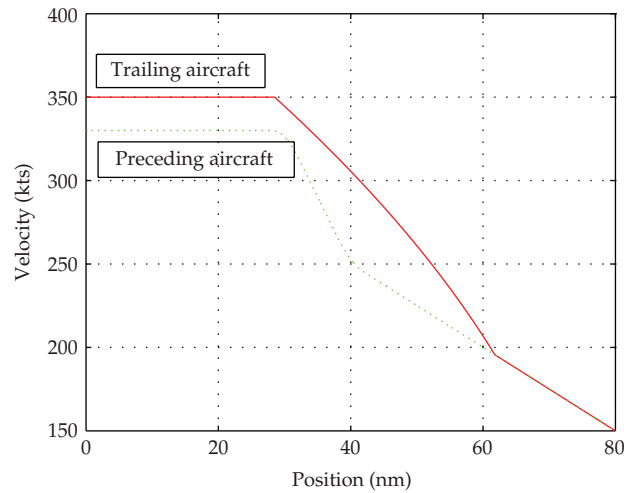
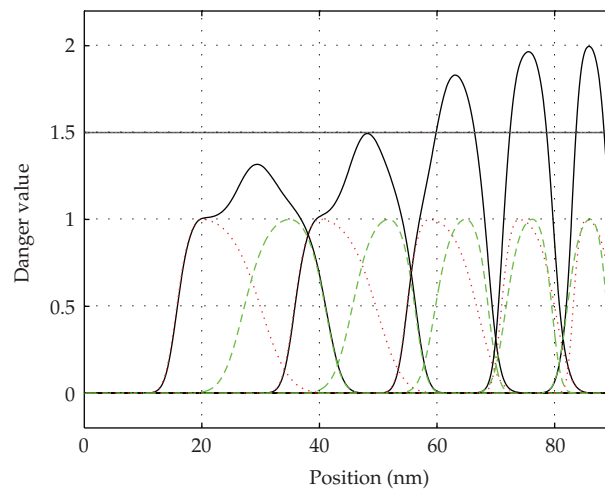**Figure 5:** Velocity profiles of the trailing and preceding aircraft.



**Figure 6:** Danger value flow without velocity adjustment.

Here, we present a scenario in which a small aircraft is following a B757 aircraft during the landing process. Figure 6 illustrates the result of the combined danger value distributions at different time steps in a single figure. The danger value distribution at each time step is shown as solid-line curves. As shown in this figure, the combined danger value increases as the distance between the two aircraft decreases. Eventually, the combined danger value exceeds the critical value of 1.5, which indicates that there is insufficient time-based separation between these two aircraft. Figure 7 shows the result obtained after applying the proposed velocity adjustment procedure presented in Section 3. As shown in this figure, the combined danger value increases with time until the peak value reaches the critical value of 1.5. However, in this case, the peak danger value remains at the critical value of 1.5. This means that by using the proposed speed adjustment procedure, the minimally required time-based separation can be maintained.
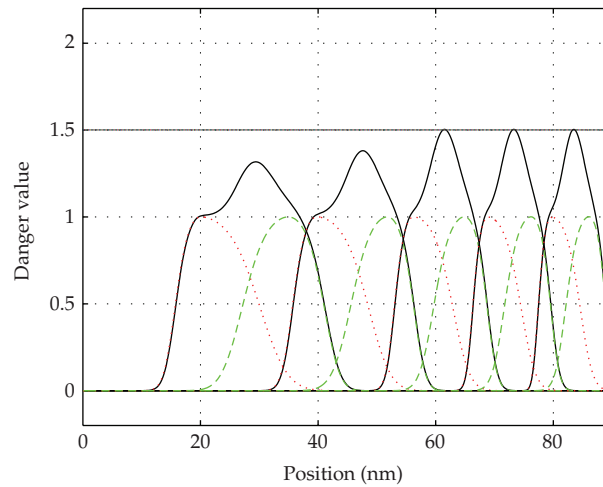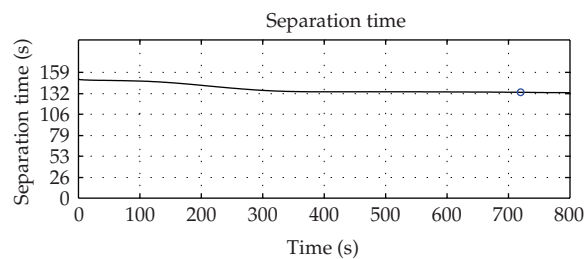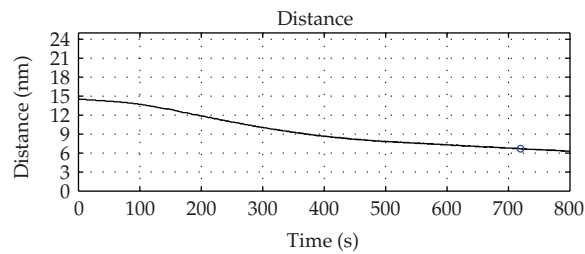
**Figure 7:** Danger value flow with velocity adjustment.



(a)



(b)

**Figure 8:** Separation in seconds and nautical miles.

To better illustrate the actual separation condition between these aircraft, the separation distance and time are shown in Figure 8. In this figure, the separation time decreases at the beginning and stops decreasing when its value reaches the minimum separation time, which is 132 s. It should also be noted that the separation distance continues to decrease because these two aircraft are decelerating. The final separation distance is greater than ICAO's separation criteria because the trailing aircraft flies with a speed greater than the average landing speed used to generate the time-based separation criteria.

The total computation time for the separation detection process as well as the speed adjustment process, determined using a laptop with Intel i5 M540 CPU and 6 GB of RAM,

was 1.8 s, which is not short enough for real-time applications. However, as the change in the velocity profile usually does not occur at the beginning of the landing process, 1.8 s of computation time may still be acceptable. Moreover, the code for computation can be further optimized using parallel computation for each aircraft and loop unfolding. Therefore, the computation time can be further reduced for real applications.

## 5. Conclusions

This study presented a flow model that uses the danger value distribution to represent possible dangers of collision surrounding each aircraft on an airway. Overlapping of the danger value distributions of each aircraft on the route can indicate the level of the time-based separation. This method can be used as an indicator of insufficient time-based separation. With the proposed flow model, a velocity adjustment algorithm using the deceleration of the trailing aircraft was presented in this paper. Using the proposed algorithm, the trailing aircraft can decelerate according to its capabilities. The modified velocity profile of the trailing aircraft can be used to maintain the separation time at its minimum required value and thus can better utilize the capacity of an airway.

Through the development of danger value profiles, we demonstrated that both the forward and backward danger value profiles have practical importance. Different danger value profiles can be constructed for various types of aircraft, and a more sophisticated time-based separation can be applied to further optimize the usage of limited runway/airport capacity. Apart from the influence of wake vortices, the estimation error of aircraft positions can also be included into our method. The danger value distribution can be modified or expanded to incorporate the estimation error of aircraft position. In the future, the study of how the estimation error affects the danger value profile will be pursued.

## Acknowledgment

## References

[1] E. Freville and J.-P. Nicolaon, "Potential benefits of a time-based separation procedure to maintain the arrival capacity of an airport in strong head-wind condictions," in *Proceedings of the 5th USA/Europe Air Traffic Management Research and Development Seminar*, 2003.

[2] M. Janic, "Toward time-based separation rules for landing aircraft," *Journal of the Transportation Research Record*, no. 2052, pp. 79–89, 2008.

[3] J. Abela, D. Abramson, M. Krishnamoorthy, A. D. Silva, and G. Mills, "Computing optimal schedules for landing aircraft," in *Proceedings of the 12th National Conference of the Australian Society for Operations Research*, pp. 71–90, July 1993.

[4] L. Bianco, P. Dell'Olmo, and A. R. Odoni, *Modelling and Simulation in Air Traffic Management*, Springer, New York, NY, USA, 1997.

[5] J. E. Beasley, M. Krishnamoorthy, Y. M. Sharaiha, and D. Abramson, "Scheduling aircraft landings—the static case," *Transportation Science*, vol. 34, no. 2, pp. 180–197, 2000.

[6] J. E. Beasley, M. Krishnamoorthy, Y. M. Sharaiha, and D. Abramson, "Displacement problem and dynamically scheduling aircraft landings," *Journal of the Operational Research Society*, vol. 55, no. 1, pp. 54–64, 2004.

[7]  H. Helmke, R. Hann, M. Uebbing-Rumke, D. Müller, and D. Wittkowski, "Time-based arrival management for dual threshold operation and continous descent approaches," in *Proceedings of the 8th USA/Europe Air Traffic Management Research and Development Seminar*, 2009.

[8]  M. J. Lighthill and G. B. Whitham, "On kinematic waves. I. Flood movement in long rivers," *Proceedings of the Royal Society A*, vol. 229, pp. 281–316, 1955.

[9]  M. J. Lighthill and G. B. Whitham, "On kinematic waves. II. A theory of traffic flow on long crowded roads," *Proceedings of the Royal Society A*, vol. 229, pp. 317–345, 1955.

[10]  P. I. Richards, "Shock waves on the highway," *Operations Research*, vol. 4, pp. 42–51, 1956.

[11]  L. Leclercq, "Hybrid approaches to the solutions of the "Lighthill-Whitham-Richards" model," *Transportation Research B*, vol. 41, no. 7, pp. 701–709, 2007.

[12]  D. Sun, I. S. Strub, and A. M. Bayen, "Comparison of the performance of four Eulerian network flow models for strategic air traffic management," *Networks and Heterogeneous Media*, vol. 2, no. 4, pp. 569–595, 2007.

[13]  P. K. Menon, G. D. Sweriduk, T. Lam, G. M. Diaz, and K. D. Bilimoria, "Computer-aided Eulerian air traffic flow modeling and predictive control," in *Proceedings of the Collection of Technical Papers—AIAA Guidance, Navigation, and Control Conference*, pp. 2683–2697, August 2004.

[14]  P. K. Menon, G. D. Sweriduk, and K. D. Bilimoria, "New approach for modeling, analysis, and control of air traffic flow," *Journal of Guidance, Control, and Dynamics*, vol. 27, no. 5, pp. 737–744, 2004.

[15]  P. K. Menon, G. D. Sweriduk, T. Lam, G. M. Diaz, and K. D. Bilimoria, "Computer-aided eulerian air traffic flow modeling and predictive control," *Journal of Guidance, Control, and Dynamics*, vol. 29, no. 1, pp. 12–19, 2006.

[16]  C. A. Robelin, D. Sun, G. Wu, and A. M. Bayen, "MILP control of aggregate Eulerian network airspace models," in *Proceedings of the 2006 American Control Conference*, pp. 5257–5262, June 2006.

[17]  A. M. Bayen, R. L. Raffard, and C. J. Tomlin, "Eulerian network model of air traffic flow in congested areas," in *Proceedings of the 2004 American Control Conference (AAC)*, vol. 6, pp. 5520–5526, July 2004.

[18]  A. M. Bayen, R. L. Raffard, and C. J. Tomlin, "Adjoint-based control of a new Eulerian network model of air traffic flow," *IEEE Transactions on Control Systems Technology*, vol. 14, no. 5, pp. 804–818, 2006.

[19]  A. M. Bayen, *Computational control of networks of dynamical systems: application to the national airspace system [Ph.D. dissertation]*, Stanford University, 2003.

[20]  D. Sun, S. D. Yang, I. Strub, A. M. Bayen, B. Sridhar, and K. Sheth, "Eulerian trilogy," in *Proceedings of the AIAA Guidance, Navigation, and Control Conference*, pp. 1680–1699, August 2006.